Title: Innate Reprocessability in Engineering Thermosets

Authors: Julian C. Cooper[1,2]*, Justine E. Paul[1,3]†, Nabil Ramlawi[4]†, Chaimongkol Saengow[1,4], Anisha Sharma[1,3], Benjamin A. Suslick[1,2], Randy H. Ewoldt[1,4]*, Nancy R. Sottos[1,3]*, Jeffrey S. Moore[1,2]*

Affiliations:

[1] Beckman Institute for Advanced Science and Technology, University of Illinois Urbana-Champaign, Urbana, IL 61801, USA.

[2] Department of Chemistry, University of Illinois Urbana-Champaign, Urbana, IL 61801, USA.

[3]Department of Materials Science and Engineering, University of Illinois Urbana-Champaign, Urbana, IL 61801, USA.

[4] Department of Mechanical Science and Engineering, University of Illinois Urbana-Champaign, Urbana, IL 61801, USA.

† These authors contributed equally to this work.

*Corresponding author Email: jccooper@illinois.edu, ewoldt@illinois.edu, n-sottos@illinois.edu, jsmoore@illinois.edu

Abstract:

While valued for their durability and exceptional performance, crosslinked thermosets are challenging to recycle and reuse. Here, we unveil inherent reprocessability in industrially relevant polyolefin thermosets. Unlike prior methods, our approach eliminates the need to introduce exchangeable functionality to regenerate the material, relying instead on preserving the activity of the metathesis catalyst employed in the curing reaction. Frontal ring opening metathesis polymerization (FROMP) proves critical to preserving this activity. We explore conditions controlling catalytic viability to successfully reclaim performance across multiple generations of material, thus demonstrating long-term reprocessability. This straightforward and scalable remolding strategy is poised for widespread adoption. Given the anticipated growth in polyolefin thermosets, our findings represent an important conceptual advance in the pursuit of a fully circular lifecycle for thermoset polymers.

One-Sentence Summary: By preserving metathesis catalyst activity, reprocessability of previously non-recyclable polyolefin thermosets is achieved.

Main Text:

Crosslinked thermoset polymers are prized for their mechanical properties; consequently these materials find uses in many structural and high-performance applications needed for civil, energy and transportation infrastructure (*1*). While crosslinks enhance performance, they create challenges for recyclability, often leading to the disposal or incineration of thermosets the end of their service lifetime (2, 3). Equipping thermosets with mechanisms that enable reformability without loss of mechanical properties will divert these materials from waste streams.

An attractive strategy to circularize the lifecycle of these materials is to render thermoset strands or crosslinks exchangeable, thereby reconfiguring an otherwise permanent network when certain conditions are met. This approach is capable of restoring the original thermoset properties, imbuing these covalent adaptable networks (CANs) with reprocessability akin to thermoplastics (*2–4*). A number of chemistries have been successfully implemented to achieve thermoset remodeling, giving multigenerational materials displaying wide-ranging properties (*5*). Despite the promise of this approach, introduction of new chemistry to drive exchange limits wider adoption of these materials. CANs are traditionally made by either crosslinking existing thermoplastics with exchangeable functionality (*6–8*), or by incorporating tailored monomers or crosslinkers containing exchangeable functionality during material synthesis (*9–12*). Consequently, with the exception of thermosets that already possess intrinsically exchangeable bonds (e.g. polyurethanes (*13*) and polyesters(*14*, *15*)), existing CAN materials are not readily scalable, and are ill-suited to displace existing thermosetting materials. Reprocessing industrially relevant thermosets will make the most meaningful strides towards the goal of circularizing the thermoset lifecycle. Translating CAN-like behavior into real-world materials, however, will require not only overcoming permanence imparted by their native topology, but doing so in a manner that avoids needing to incorporate new chemistry to achieve exchangeability. Remodeling using "off-the-shelf" components that are both compatible with standard processing methods and are free from complexities of new monomer functionality, will eliminate the hurdles to scalability that plague CAN materials and promote their broader adoption.

With these objectives in mind, we formulated an innate remodeling hypothesis, which if validated, would lead to straightforward, multigenerational capabilities in poly(dicyclopentadiene) (pDCPD)—a high-performance polyolefin thermoset produced annually on the multi-million metric ton scale, with excellent impact and chemical resistance, high fracture toughness and stiffness, and readily tunable properties (*16–20*). The envisioned remodeling mechanism targets cross metathesis exchange of the olefins in the backbone. Olefin metathesis has been previously implemented for network remodeling, where addition of an *exogenous* metathesis catalyst facilitates strand exchange (*21–23*). Infiltration of catalysts into thermosets is a mass-transport-limited, solvent-intensive process that becomes impractical for the mass production of large fabricated parts. The innate remodeling approach is simpler and more practical because it harnesses the same catalyst used in the metathesis-based curing reaction to facilitate subsequent exchange processes for reprocessability.

The viability of the metathesis catalyst utilized in producing the pDCPD material is crucial to the success of the proposed approach. Following high temperature isothermal curing, the catalyst is generally presumed to have greatly diminished or non-existent activity (*24*, *25*), and therefore incapable of reconfiguring the network. Here we show that this need not be the case, and maintaining catalyst activity strongly depends on the resin formulation and conditions of the curing reaction. In a recent development, our research group made the surprising observation that the molecular weight of a bulk thermoplastic produced through frontal ring-opening metathesis (FROMP) could be increased via a chain extension process under inert atmosphere.(*26*) This indicated that Grubbs 2nd generation catalyst (GC2) retains catalytic activity after FROMP. FROMP is a bulk olefin metathesis polymerization technique that leverages a monomer's enthalpy of polymerization to sustain a rapidly propagating directional front, converting an olefinic monomer into a solid polymeric material (**Fig.** 1A) (*27*, *28*). The process is energy-efficient and easily scalable, and materials manufactured by FROMP display identical mechanical properties to those prepared by conventional methods (*29*). We hypothesized that residual active catalyst present after FROMP will enable remolding of the pDCPD network through metathetic strand exchange (**Fig.** 1B). The simplicity of such strategy would render this approach readily scalable, adoptable, and translatable to engineering thermosets, unlocking a naturally "innate" reprocessability.

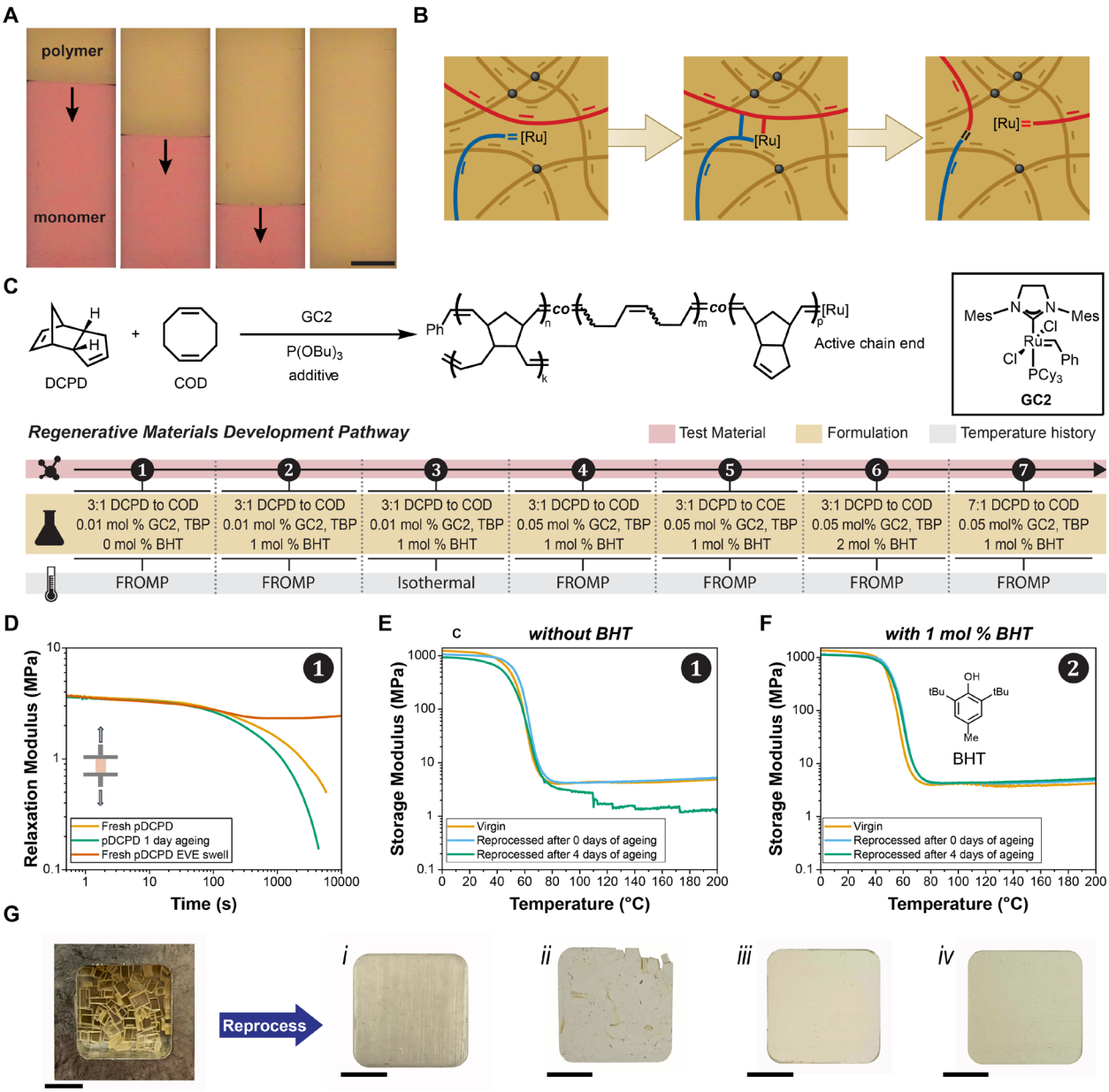

Fig. 1. Remodeling with the embedded catalyst. (**A**) A time sequence of optical images for a prototypical frontal ring opening metathesis polymerization (FROMP). For shown polymerization, front velocity = 1.1 mm/s. (**B**) Catalytic cross metathesis mechanism to enable innate remodeling (**C**) Chemical reaction for FROMP of DCPD and COD, with active catalyst chain ends (GC2 = Grubbs 2nd generation catalyst); materials development pathway showing the numerical identifiers of the formulations referred to in the manuscript (**D**) Stress relaxation of pDCPD thermoset ❶ (**E**) Representative dynamic mechanical analysis (DMA) (2.0 °C min^{-1}, 1 Hz) of ❶ immediately after FROMP (virgin), reprocessed immediately after FROMP (reprocessed) and reprocessed after four days of aging, likewise in (**F**) with pDCPD containing 1 mol% BHT (❷). *Reprocessing conditions*: 2 tons (29 MPa), 90 °C, 1 h, under N_2 atmosphere. (**G**) Images (enhanced for clarity) of reprocessed pDCPD thermosets tested, subjected to conditions listed in (E-F): reprocessed ❶ after (*i*) 0 days ageing and (*ii*) after 4 days ageing. Reprocessed ❷ after (*iii*) 0 days of ageing, and (*iv*) after 4 days ageing. *All Scalebars = 1 cm*.

To test our innate remodeling hypothesis, we introduced commercially available 1,5-cylooctadiene (COD) as a comonomer with DCPD. Not only does COD readily incorporate during

FROMP, allowing for tunable control of pDCPD thermomechanical properties (*18*), but it introduces less hindered olefins into the pDCPD network that readily participate in metathesis. While a variety of different metathesis catalyst are compatible with FROMP (*30*), the stability and ease of handling of ruthenium-based Grubbs 2nd generation catalyst (GC2) make it attractive to enable multigenerational capabilities. We frontally polymerized a neat 3:1 molar ratio of DCPD:COD under prototypical FROMP conditions: 0.01 mol% of GC2 (with respect to total moles of monomer) and 0.01 mol% tributylphosphite (TBP) as added inhibitor, making pDCPD material **1** with which to investigate catalyst-driven remolding (details about all materials referenced in text are found in **Fig.** 1C). Characterization of frontal polymerization of **1** was carried out in a test tube, but to facilitate testing of the mechanical and regenerative properties, **1** was frontally polymerized directly in 1 mm thick u-shaped gaskets (**Fig.** S3, S6-8 ***Movie*** S1).

We subjected **1** to stress relaxation experiments to test the ability of residual catalyst to promote remodeling. In stress relaxation, a fixed strain within the linear viscoelastic regime is imposed on the material, and the evolution of the resulting stress is observed. While a permanent network will not relax completely, a dynamic network will undergo remodeling to dissipate the stress imposed by this strain. Consistent with catalyst driving exchange of the network, **1** undergoes near complete relaxation at 80 °C (**Fig.** 1D, yellow). An increase in the rate of relaxation after one day in air demonstrates that the inhibitor mediates catalytic activity (**Fig.** 1D, blue), with oxidation of TBP to the phosphate ester placing a larger fraction of the catalyst in the active state. Importantly, **1** loses the ability to relax when swelled with ethyl vinyl ether (EVE) used to deactivate the catalyst (**Fig.** 1D, red), with the material assuming characteristics of a permanent network. These experiments are consistent with the catalyst retaining activity in the thermoset after FROMP. Given these findings, we proceeded to investigate the ability of the catalyst to affect macroscopic remodeling. We pelletized and compression molded thermoset **1** to reform a new monolith (**Fig.** 1E. 1Gi). Dynamic mechanical analysis (DMA) reveals that the remolded monolith exhibits near identical thermomechanical properties as the original **1**. In line with the stress relaxation experiments, reprocessing of **1** swollen in EVE failed to regenerate effectively and recover original properties (**Fig** S10-11). Combined, these experiments implicate the catalyst as being responsible for remodeling the network material.

Critical to multigenerational capabilities is preservation of reconfigurability over time. After four days, **1** could no longer reprocess and maintain comparable properties to the original thermoset (**Fig.** 1E, 1G*ii* and **Fig.** S12). We postulated that this loss in network remoldability was due to either O_2 promoted oxidative crosslinking of the polyolefin material or catalyst death. Oxidative ageing plagues many commodity materials, but can be suppressed by introduction of antioxidants (*31*). To preserve remoldability, 1 mol% butylated hydroxytoluene (BHT) was added to an otherwise identical 3:1 DCPD:COD formulation (**2**). Introduction of BHT did not interfere with the ability to frontally polymerize, and compared to **1**, the resulting **2** maintains its thermomechanical properties over the same period (**Fig.** 1F, 1G*iii-iv*).

We proceeded to subject **2** to stress relaxation experiments at increasing temperatures to gain insights into the remodeling and viscoelastic behavior of this pDCPD thermoset. We extracted a characteristic relaxation time, τ, based on the time to relax to $1/e$ of the initial modulus, which captures the dominant exponential decay mode. Sweeping from 80 °C to 110 °C in an N_2 environment, we observed exponential decrease in $\tau(T)$, consistent with higher catalytic activity with increasing temperature and near complete dissipation of the imposed stress (**Fig.** 2A). Over this temperature range, τ follows Arrhenius-like behavior (**Fig.** 2B, S14). However, in progressing to higher temperatures, we observe an attenuation in the rate of relaxation, and at 140 ºC the

characteristic relaxation time is slower than that seen at lower temperatures. The starting modulus at 140 °C is nearly identical to moduli at lower temperatures (**Fig.** S15), suggesting that a change of network structure is not responsible for the observed slowdown in relaxation behavior. Instead, it implies that the active catalyst in the material is undergoing temperature-dependent deactivation.

The temperature-dependent network dynamics imply that the curing process used for the initial resin significantly impacts the preservation of catalyst viability. In conventional curing techniques, the DCPD resin is heated at elevated temperatures for extended times (*29*). By contrast, in FROMP, the resin experiences a brief temperature spike as the front passes. We hypothesized that this rapid FROMP curing preserves catalytic activity and imparts pDCPD with multigenerational capabilities. We aimed to test this prediction by comparing the dynamic remodeling capabilities of our thermoset made by FROMP to an otherwise identical thermoset made by conventional methods. A number of different curing cycles have been reported to manufacture pDCPD (*32–34*), but for a representative comparison, we chose a 30-min isothermal cure cycle at 120 °C under an atmosphere of N_2, generating ❸. In line with this hypothesis, τ of ❸ at reprocessing temperatures of 90 °C is approximately four times longer than ❷ (**Fig.** 2C). Furthermore, heating of ❷ for 2 h under isothermal curing conditions leads to near complete loss of relaxation (**Fig.** S16). These findings are consistent with creep experiments to observe vitrified flow (**Fig**. 2D), which show that ❸ possesses nearly two orders of magnitude higher viscosity than ❷ (**Table** S5)**,** indicative of more active catalyst present in the FROMP material. DMA further supports this notion, where both virgin ❷ and ❸ display similar thermomechanical properties, but only ❷ successfully recovers the original thermomechanical properties when reprocessed (**Fig.** 2E), with poor remodeling seen for ❸. These differences showcase the capability and promise of FROMP to function as a key enabling technology for the manufacturing of multigenerational pDCPD thermosets in a readily scalable manner.

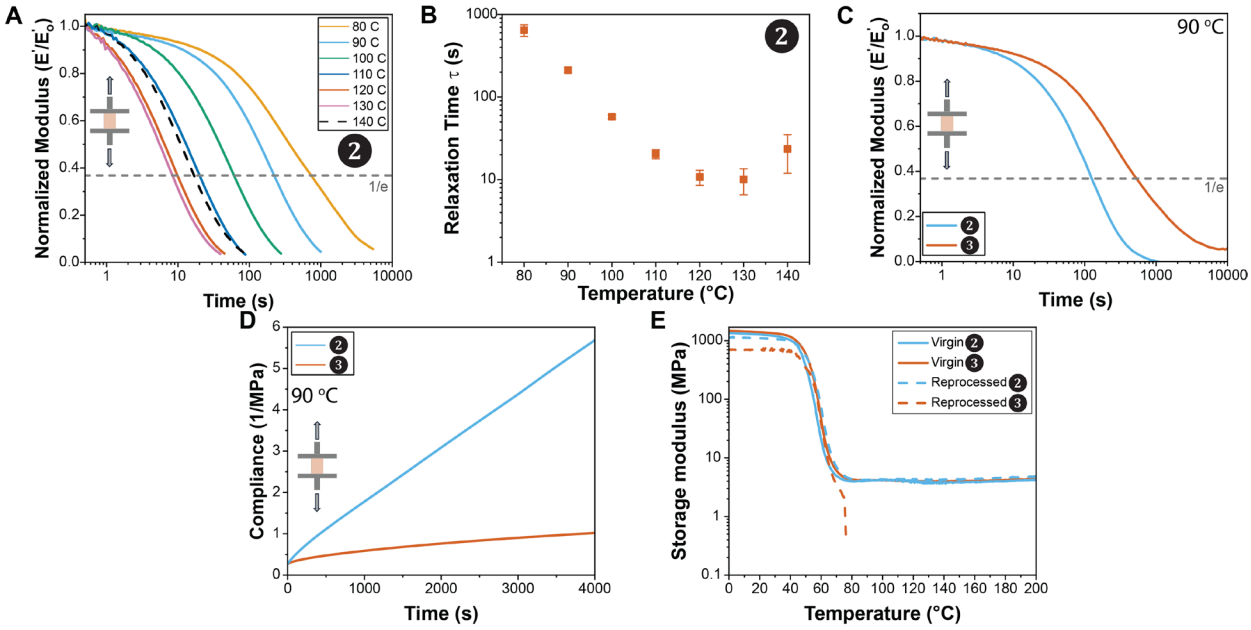

Fig. 2. FROMP –not isothermal curing– maintains catalyst activity. (**A**) Stress relaxation temperature sweep of pDCPD ❷, with generally faster relaxation rate seen at higher temperatures. (**B**) Evolution of relaxation time with temperature (**C**) Stress relaxation of pDCPD thermoset made by FROMP and isothermal-curing. *Isothermal curing conditions*: 120 °C, 30 min, N_2 atmosphere (**D**) Compliance from creep experiments of ❷ and ❸. (**E**) Thermomechanical properties of ❷ and ❸, compared to recovered properties after first reprocessing. *Formulations numbers correspond to those in* ***Fig.*** *1*

Maintaining catalyst viability is critical to sustained reprocessability, and after just 8 days, ❷ also loses much of its ability to remodel (**Fig.** S13). Increasing GC2 loading in the resin represents a simple strategy to extend pDCPD reprocessability. In fact, we found that pDCPD ❹ containing 0.05 mol% catalyst exhibits prolonged reprocessability (*vide infra*). We conducted a series of sequential stress relaxation experiments on ❹, monitoring the evolution in τ with both time and temperature. Because these experiments are run in a controlled N_2 environment and no other mechanisms to affect network topology are present, any observed changes in τ will directly correlate to changes in catalytic activity. A representative set of consecutive stress relaxation experiments is depicted in **Fig.** 3A. Compared to the initial characteristic relaxation time τ_o, a near 3-fold increase in τ for ❹ is seen over the course of 42 min at 120 °C. Analysis of the characteristic relaxation times at different temperatures provides an in-depth look at how catalyst deactivation depends on temperature (**Fig.** 3B). At reprocessing temperatures of 90 °C virtually no change in τ was observed. Conversely at 130 °C, the characteristic time τ lengthened rapidly (τ_o/τ decreases).

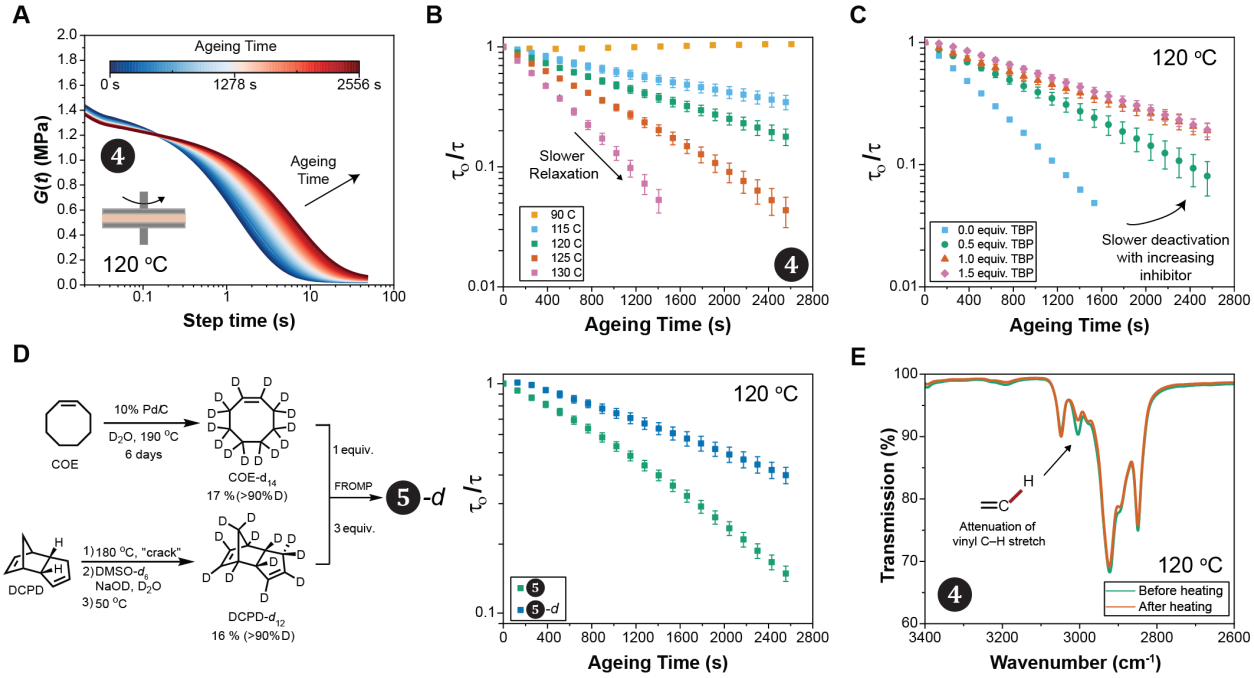

Fig. 3. Probing catalyst deactivation. (**A**) Representative isothermal evolution of the relaxation modulus $G(t)$ for pDCPD thermoset ❹ at the same temperature. *See supplementary information for details.* (**B**) Rate of change of the characteristic relaxation time at different temperatures in freshly prepared pDCPD material. (**C**) Role of increasing amounts of tributylphosphite (TBP) on the catalyst viability in the network. (**D**) Preparation of deuterated pDCPD material ❺-*d* and comparison of its decay to its ^{1}H analogue ❺. (**E**) IR spectrum of ❹ showing the C–H stretch region before and after heating the material at 120 °C for 2 h. *Formulations numbers correspond to those in* ***Fig.*** *1*

We next sought to gain insight into the mechanism of this temperature-promoted catalyst deactivation. Ruthenium-based catalysts are known to undergo deactivation by various pathways (*35*), and establishing the predominant pathway for catalyst deactivation will provide insights to enhance catalyst lifetime. Bimolecular pathways proceeding *via* catalyst-catalyst interactions are unlikely given both low catalyst loadings, and more limited catalyst diffusion in the thermoset compared to solution (*36*). The faster increase in τ for ❷ compared to ❹ is opposite of what would be expected for a bimolecular catalyst-catalyst deactivation pathway (**Fig.** S29).

Furthermore, an Eyring analysis applied to **Fig** 3B indicates deactivation is first order in catalyst concentration (**Fig.** S30-32). Phosphines are known to promote catalyst deactivation *via* nucleophilic addition to the Ru carbene, and we anticipate the phosphite inhibitor added to facilitate resin handling could similarly accelerate catalyst deactivation (*37*). However, we found the opposite to be true. Specifically, when we monitored relaxation behavior with different phosphite loadings at 120 °C, the rate of change in τ decreased with *increasing* TBP loading (**Fig.** 3C). Conversely, oxidation of the TBP to the corresponding P=O by exposure of **4** to air for 5 days resulted in a faster rate of change in τ (**Fig.** S42). Furthermore, BHT did not accelerate the evolution of τ, indicating that BHT plays little role in catalyst decomposition (**Fig**. S46). Taken together, these results suggest that catalyst deactivation in the material arises from an intermediate intimately associated with the catalytically active species.

Substrate-mediated catalyst deactivation in the context of small molecule substrates proceeds *via* a β-hydride-elimination from the Ru-metallacyclobutane intermediate, leading to loss of the active ruthenium carbene (*38–41*). We synthesized **5**-*d*, a perdeuterated analogue of **4**, composed of 75 mol% DCPD-d_{12}, 25 mol% cyclooctene-d_{14} (COE-d_{14}), and 1 mol% BHT, to test whether such decomposition is operative in our material (**Fig.** 3D). When subjected to repeated stress relaxation, the evolution of τ for **5**-*d* was nearly 2 times slower than that of **5** at 120 ºC (**Fig.** 3D, **Fig.** S47-48), indicative of a strong isotope effect associated with catalyst deactivation and consistent with β-hydride-elimination. Further supporting a β-hydride-mediated decomposition, IR spectroscopy shows an attenuation of the vinyl (=C–H) stretching mode (3008 cm^{-1}) of **4** after being heated at 120 °C for 2 h (**Fig**. 3E, Fig. S53-55) Experiments with materials of hybrid deuteration (e.g., DCPD-d_{12}: COE-h_{14}) reveal that β-hydride abstraction primarily arises from the COE fragment (**Fig.** S51). These observations also indicate that other known deactivation pathways, such as C–H insertion into the NHC ligand, are not significant contributors (*42*). Substrate-catalyst deactivation pathways imply catalyst stability depends on the composition the material; for example, **5** undergoes deactivation at a faster rate when compared to **4** (**Fig.** S59). This understanding highlights the importance of different catalyst features in network remodeling, and motivates the need for more resilient catalysts for multigenerational thermosets.

Cognizant of the factors influencing catalyst viability, we set out to illustrate extended reprocessability in our pDCPD thermosets. Compression molding of pelletized **4**, under 2 tons of force (29 MPa) and N_2 at 90 ºC for 1 hour generated a monolith of **4**·**R1**: a second-generation material of **4** (**Fig.** 4A). We subsequently reprocessed **4**·**R1** an additional two times, yet sequential stress relaxation of **4** showed near zero change in τ_o/τ over the combined time of three reprocessing cycles, suggesting further generations are accessible (**Fig.** S71). Effective recovery of thermomechanical properties is achieved across all generations of **4** tested (**Fig.** 4B). Remarkably, even after 50 days, we were able to reprocess and recover thermomechanical properties of the original material **4** (**Fig.** 4C). We hypothesized increasing BHT loading may serve to further extend reprocessability. We found pDCPD **6** containing 2 mol% BHT exhibited a slower rate of mutation in τ compared to **4** after ageing for the same duration, indicating that BHT preserves active catalyst in the material (**Fig.** S73). Further supporting this hypothesis, 50-day-aged **6** effectively recover its original mechanical properties when reprocessed, giving a new monolith with fewer defects compared to **4** (**Fig**. S84-85).

This remodeling approach is readily translatable to other polyolefins made by FROMP. Material properties were effectively recovered in thermosets displaying both higher and lower glass transition temperatures (T_g) (**Fig.** S86-87). In fact, we were even able to reprocess materials

approaching T_g of native pDCPD: the thermomechanical properties of pDCPD **7** (T_g 110 °C) were successfully recovered (**Fig.** 4D). However, the temperature required to successfully reprocess this material (130 °C) coincided with the temperatures at which catalyst undergoes rapid deactivation (*vide supra*). Consequently, further generations of **7** proved inaccessible (**Fig.** S88), further motivating the need for catalysts with prolonged high thermal stability.

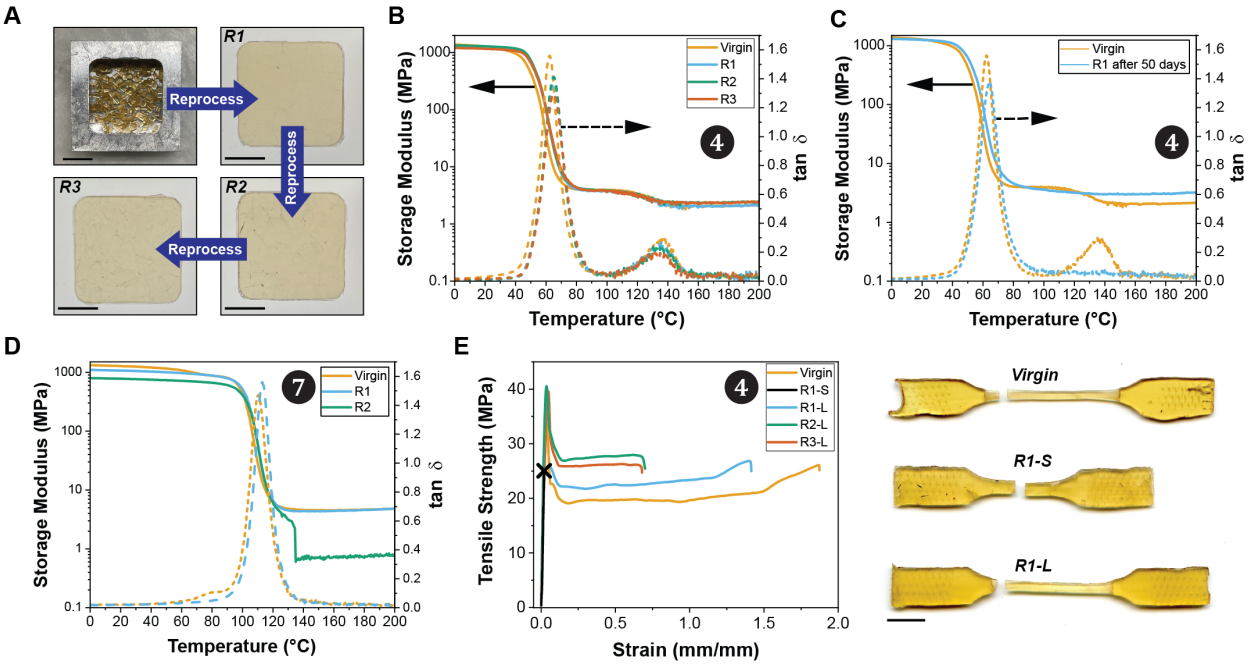

Fig. 4. Probing pDPCD performance across multiple material generations. (**A**) Representative optical images of subsequent generations of pDCPD material fabricated by reprocessing pellets of the prior generation (R# = number of times reprocessed). Reprocessing conditions: 2 tons (29 MPa), 90 °C, 1 h, under N_2 atmosphere. (**B**) Dynamic mechanical analysis (DMA) of different material generations, storage modulus (left, solid) and tan δ (right, dashed). (**C**) Thermomechanical properties of a reprocessed specimen after 50 days of sitting in ambient conditions as compared to a virgin specimen. (**D**) Dynamic mechanical analysis of pDCPD specimen displaying high performance, and recovery of those properties across multiple generations. (**E**) Representative stress-strain curves (5 mm min^{-1}) for different material generations reprocessed from small (S) and large (L) pellets (*See supplementary information*), and images of failed tensile specimens showing the resulting failure modes. *Scalebars = 1cm. Formulations numbers correspond to those in* ***Fig.*** *1*

We evaluated effective recovery of pDCPD *performance* using uniaxial tensile measurements. Virgin **4** exhibited an elastic modulus of 1.24 ± 0.16 GPa and yield strength of 32.8 ± 1.26 MPa, along with cold-drawing behavior before failure (**Fig.** 4E), characteristic of pDCPD materials (*16*). Testing of the material compression molded from small pellets led to good recovery of elastic modulus, but decreased yield strength with brittle fracture (**R1-S**). This loss of mechanical properties is likely due to mechanical breakdown or oxidation of the network strands during breakdown of the material into high surface-to-volume ratio pellets. While catalyst mediated remodeling alters the local connectivity of these smaller strands to each other, olefin cross metathesis is incapable of repairing damage from homolytic C–C bond cleavage of the network strands caused by this breakdown.(*43*) By contrast, larger pellets (**Fig.** S89) of **4** reprocessed under otherwise identical conditions leads to full reclamation of material performance over multiple material generations (**Reprocessing-L**). Both linear and non-linear material behavior were recovered, consistent with the parent network having undergone fewer irrecoverable

bond scission events during reprocessing. These differences in recovered properties point to the importance of detailing the conditions of the material being reprocessed.

In summary, our findings challenge the conventional belief that the catalyst used to manufacture polyolefin thermosets inevitably lose their activity after curing. We demonstrate their remarkable ability not only to create but also to regenerate the material. The rapid curing profile of FROMP is key to unlocking these regenerative capabilities by preserving the catalyst in the thermoset. This preservation of catalytic activity is critical for continued reprocessability. We bridge mechanistic chemical understanding with mechanics to elucidate the features governing catalyst lifetime in the material once it is made. This work not only motivates future catalyst development, including the exploration of more thermally stable catalysts, but also introduces intriguing possibilities. These include the potential for reversible switching of catalyst activity "on" and "off" through an environmental stimulus. This could address issues like the undesirable creep typical of CAN materials or open doors to thermoset deconstruction via metathetic alkenolysis (*44*). The simplicity of the innate remodeling approach allows for its transferability to other polyolefins, advancing scalable end-of-life management strategies for a wide range of real-world engineering materials.

References and Notes

1. J.-P. Pascault, H. Sautereau, J. Verdu, R. J. J. Williams, *Thermosetting Polymers* (CRC Press, New York, ed. 1st, 2002).
2. C. J. Kloxin, T. F. Scott, B. J. Adzima, C. N. Bowman, Covalent Adaptable Networks (CANs): A Unique Paradigm in Cross-Linked Polymers. *Macromolecules*. **43**, 2643–2653 (2010).
3. B. R. Elling, W. R. Dichtel, Reprocessable Cross-Linked Polymer Networks: Are Associative Exchange Mechanisms Desirable? *ACS Cent. Sci.* **6**, 1488–1496 (2020).
4. D. J. Fortman, J. P. Brutman, G. X. De Hoe, R. L. Snyder, W. R. Dichtel, M. A. Hillmyer, Approaches to Sustainable and Continually Recyclable Cross-Linked Polymers. *ACS Sustainable Chem. Eng.* **6**, 11145–11159 (2018).
5. G. M. Scheutz, J. J. Lessard, M. B. Sims, B. S. Sumerlin, Adaptable Crosslinks in Polymeric Materials: Resolving the Intersection of Thermoplastics and Thermosets. *J. Am. Chem. Soc.* **141**, 16181–16196 (2019).
6. F. Caffy, R. Nicolaÿ, Transformation of polyethylene into a vitrimer by nitroxide radical coupling of a bis-dioxaborolane. *Polym. Chem.* **10**, 3107–3115 (2019).
7. M. Röttger, T. Domenech, R. van der Weegen, A. Breuillac, R. Nicolaÿ, L. Leibler, High-performance vitrimers from commodity thermoplastics through dioxaborolane metathesis. *Science*. **356**, 62–65 (2017).
8. J. J. Lessard, K. A. Stewart, B. S. Sumerlin, Controlling Dynamics of Associative Networks through Primary Chain Length. *Macromolecules*. **55**, 10052–10061 (2022).
9. J. S. A. Ishibashi, J. A. Kalow, Vitrimeric Silicone Elastomers Enabled by Dynamic Meldrum's Acid-Derived Cross-Links. *ACS Macro Lett.* **7**, 482–486 (2018).
10. W. Denissen, G. Rivero, R. Nicolaÿ, L. Leibler, J. M. Winne, F. E. Du Prez, Vinylogous Urethane Vitrimers. *Advanced Functional Materials*. **25**, 2451–2457 (2015).
11. J. J. Lessard, G. M. Scheutz, R. W. Hughes, B. S. Sumerlin, Polystyrene-Based Vitrimers: Inexpensive and Recyclable Thermosets. *ACS Appl. Polym. Mater.* **2**, 3044–3048 (2020).
12. K. E. L. Husted, C. M. Brown, P. Shieh, I. Kevlishvili, S. L. Kristufek, H. Zafar, J. V. Accardo, J. C. Cooper, R. S. Klausen, H. J. Kulik, J. S. Moore, N. R. Sottos, J. A. Kalow, J. A.

Johnson, Remolding and Deconstruction of Industrial Thermosets via Carboxylic Acid-Catalyzed Bifunctional Silyl Ether Exchange. *J. Am. Chem. Soc.* **145**, 1916–1923 (2023).
13. D. J. Fortman, J. P. Brutman, C. J. Cramer, M. A. Hillmyer, W. R. Dichtel, Mechanically Activated, Catalyst-Free Polyhydroxyurethane Vitrimers. *J. Am. Chem. Soc.* **137**, 14019–14022 (2015).
14. D. Montarnal, M. Capelot, F. Tournilhac, L. Leibler, Silica-Like Malleable Materials from Permanent Organic Networks. *Science*. **334**, 965–968 (2011).
15. J. L. Self, N. D. Dolinski, M. S. Zayas, J. Read de Alaniz, C. M. Bates, Brønsted-Acid-Catalyzed Exchange in Polyester Dynamic Covalent Networks. *ACS Macro Lett.* **7**, 817–821 (2018).
16. D. G. Ivanoff, J. Sung, S. M. Butikofer, J. S. Moore, N. R. Sottos, Cross-Linking Agents for Enhanced Performance of Thermosets Prepared via Frontal Ring-Opening Metathesis Polymerization. *Macromolecules*. **53**, 8360–8366 (2020).
17. J. Chen, F. P. Burns, M. G. Moffitt, J. E. Wulff, Thermally Crosslinked Functionalized Polydicyclopentadiene with a High T_g and Tunable Surface Energy. *ACS Omega*. **1**, 532–540 (2016).
18. L. M. Dean, Q. Wu, O. Alshangiti, J. S. Moore, N. R. Sottos, Rapid Synthesis of Elastomers and Thermosets with Tunable Thermomechanical Properties. *ACS Macro Lett.* **9**, 819–824 (2020).
19. K. E. L. Husted, P. Shieh, D. J. Lundberg, S. L. Kristufek, J. A. Johnson, Molecularly Designed Additives for Chemically Deconstructable Thermosets without Compromised Thermomechanical Properties. *ACS Macro Lett.* **10**, 805–810 (2021).
20. E. M. Lloyd, J. C. Cooper, P. Shieh, D. G. Ivanoff, N. A. Parikh, E. B. Mejia, K. E. L. Husted, L. C. Costa, N. R. Sottos, J. A. Johnson, J. S. Moore, Efficient Manufacture, Deconstruction, and Upcycling of High-Performance Thermosets and Composites. *ACS Appl. Eng. Mater.* **1**, 477–485 (2023).
21. Y.-X. Lu, F. Tournilhac, L. Leibler, Z. Guan, Making Insoluble Polymer Networks Malleable via Olefin Metathesis. *J. Am. Chem. Soc.* **134**, 8424–8427 (2012).
22. Y.-X. Lu, Z. Guan, Olefin Metathesis for Effective Polymer Healing via Dynamic Exchange of Strong Carbon–Carbon Double Bonds. *J. Am. Chem. Soc.* **134**, 14226–14231 (2012).
23. H. Liu, A. Z. Nelson, Y. Ren, K. Yang, R. H. Ewoldt, J. S. Moore, Dynamic Remodeling of Covalent Networks via Ring-Opening Metathesis Polymerization. *ACS Macro Lett.* **7**, 933–937 (2018).
24. S. Wolf, H. Plenio, On the ethenolysis of natural rubber and squalene. *Green Chem.* **13**, 2008–2012 (2011).
25. M. Bell, H. G. Hester, A. N. Gallman, V. Gomez, J. Pribyl, G. Rojas, A. Riegger, T. Weil, H. Watanabe, Y. Chujo, K. B. Wagener, Bulk Acyclic Diene Metathesis Polycondensation. *Macromolecular Chemistry and Physics*. **220**, 1900223 (2019).
26. D. M. Alzate-Sanchez, C. H. Yu, J. J. Lessard, J. E. Paul, N. R. Sottos, J. S. Moore, Rapid Controlled Synthesis of Large Polymers by Frontal Ring-Opening Metathesis Polymerization. *Macromolecules*. **56**, 1527–1533 (2023).
27. A. Mariani, S. Fiori, Y. Chekanov, J. A. Pojman, Frontal Ring-Opening Metathesis Polymerization of Dicyclopentadiene. *Macromolecules*. **34**, 6539–6541 (2001).
28. B. A. Suslick, J. Hemmer, B. R. Groce, K. J. Stawiasz, P. H. Geubelle, G. Malucelli, A. Mariani, J. S. Moore, J. A. Pojman, N. R. Sottos, Frontal Polymerizations: From Chemical Perspectives to Macroscopic Properties and Applications. *Chem. Rev.* **123**, 3237–3298 (2023).

29. I. D. Robertson, M. Yourdkhani, P. J. Centellas, J. E. Aw, D. G. Ivanoff, E. Goli, E. M. Lloyd, L. M. Dean, N. R. Sottos, P. H. Geubelle, J. S. Moore, S. R. White, Rapid energy-efficient manufacturing of polymers and composites via frontal polymerization. *Nature*. **557**, 223–227 (2018).
30. B. A. Suslick, K. J. Stawiasz, J. E. Paul, N. R. Sottos, J. S. Moore, Survey of Catalysts for Frontal Ring-Opening Metathesis Polymerization. *Macromolecules*. **54**, 5117–5123 (2021).
31. W. A. Yehye, N. A. Rahman, A. Ariffin, S. B. Abd Hamid, A. A. Alhadi, F. A. Kadir, M. Yaeghoobi, Understanding the chemistry behind the antioxidant activities of butylated hydroxytoluene (BHT): A review. *European Journal of Medicinal Chemistry*. **101**, 295–312 (2015).
32. P. Shieh, W. Zhang, K. E. L. Husted, S. L. Kristufek, B. Xiong, D. J. Lundberg, J. Lem, D. Veysset, Y. Sun, K. A. Nelson, D. L. Plata, J. A. Johnson, Cleavable comonomers enable degradable, recyclable thermoset plastics. *Nature*. **583**, 542–547 (2020).
33. D. R. Kelsey, D. L. Handlin Jr., M. Narayana, B. M. Scardino, In situ catalyst systems for ring-opening metathesis polymerization. *Journal of Polymer Science Part A: Polymer Chemistry*. **35**, 3027–3047 (1997).
34. H.-G. Kim, H. J. Son, D.-K. Lee, D.-W. Kim, H. J. Park, D.-H. Cho, Optimization and analysis of reaction injection molding of polydicyclopentadiene using response surface methodology. *Korean J. Chem. Eng.* **34**, 2099–2109 (2017).
35. M. Jawiczuk, A. Marczyk, B. Trzaskowski, Decomposition of Ruthenium Olefin Metathesis Catalyst. *Catalysts*. **10**, 887 (2020).
36. G. A. Bailey, M. Foscato, C. S. Higman, C. S. Day, V. R. Jensen, D. E. Fogg, Bimolecular Coupling as a Vector for Decomposition of Fast-Initiating Olefin Metathesis Catalysts. *J. Am. Chem. Soc.* **140**, 6931–6944 (2018).
37. S. H. Hong, A. G. Wenzel, T. T. Salguero, M. W. Day, R. H. Grubbs, Decomposition of Ruthenium Olefin Metathesis Catalysts. *Journal of the American Chemical Society*. **129**, 7961–7968 (2007).
38. D. Bourgeois, A. Pancrazi, S. P. Nolan, J. Prunet, The Cl2(PCy3)(IMes)Ru(□CHPh) catalyst: olefin metathesis versus olefin isomerization. *Journal of Organometallic Chemistry*. **643–644**, 247–252 (2002).
39. W. Janse Van Rensburg, P. J. Steynberg, W. H. Meyer, M. M. Kirk, G. S. Forman, DFT Prediction and Experimental Observation of Substrate-Induced Catalyst Decomposition in Ruthenium-Catalyzed Olefin Metathesis. *J. Am. Chem. Soc.* **126**, 14332–14333 (2004).
40. J. Engel, W. Smit, M. Foscato, G. Occhipinti, K. W. Törnroos, V. R. Jensen, Loss and Reformation of Ruthenium Alkylidene: Connecting Olefin Metathesis, Catalyst Deactivation, Regeneration, and Isomerization. *J. Am. Chem. Soc.* **139**, 16609–16619 (2017).
41. F. C. Courchay, J. C. Sworen, I. Ghiviriga, K. A. Abboud, K. B. Wagener, Understanding Structural Isomerization during Ruthenium-Catalyzed Olefin Metathesis: A Deuterium Labeling Study. *Organometallics*. **25**, 6074–6086 (2006).
42. S. H. Hong, M. W. Day, R. H. Grubbs, Decomposition of a Key Intermediate in Ruthenium-Catalyzed Olefin Metathesis Reactions. *J. Am. Chem. Soc.* **126**, 7414–7415 (2004).
43. W. Kauzmann, H. Eyring, The Viscous Flow of Large Molecules. *J. Am. Chem. Soc.* **62**, 3113–3125 (1940).
44. J. Bidange, C. Fischmeister, C. Bruneau, Ethenolysis: A Green Catalytic Tool to Cleave Carbon–Carbon Double Bonds. *Chemistry – A European Journal*. **22**, 12226–12244 (2016).
45. T. M. Miller, T. J. McCarthy, G. M. Whitesides, Deuterium-labeling experiments relevant to the mechanism of platinum-catalyzed hydrogenation of (diolefin)dialkylplatinum(II)

complexes: evidence for isotopic exchange via platinum surface hydrogen. The stereochemistry of reduction. *J. Am. Chem. Soc.* **110**, 3156–3163 (1988).
46. S. Matsubara, K. Asano, Y. Kajita, M. Yamamoto, C-H Bond Activation by Water on a Palladium or Platinum Metal Surface. *Synthesis*. **2007**, 2055–2059 (2007).
47. M. Mours, H. H. Winter, Time-resolved rheometry. *Rheol Acta*. **33**, 385–397 (1994).
48. S. Seabold, J. Perktold, "Statsmodels: Econometric and Statistical Modeling with Python" in *Proceedings of the 9th Python in Science Conference*, S. van der Walt, J. Millman, Eds. (2010), pp. 92–96.

Acknowledgments: The authors thank the Beckman Institute for Advance Science and Technology, the Frederick Seitz Materials Research Laboratory, and the School of Chemical Science, the School of Chemical Science NMR Laboratory, and Mass Spectrometry laboratory, all at UIUC for facilities and support to conduct this research. The authors thank Dorothy Loudermilk for assistance in preparation of Figure 1. We thank Prof. Denmark for use of his ATR-IR spectrometer. JCC thanks Dr. J. Lessard for helpful discussions during preparation of this work, as well as M. Chiu in final copy editing. J.C.C and C.S. thank the A. O. Beckman foundation for a postdoctoral fellowship, J.E.P. thanks the same foundation for a graduate fellowship.

Funding:

Air Force Office of Scientific Research (Center of Excellence in Self-Healing, Regeneration, and Structural Remodeling): FA9550-20-1-0194.

Author contributions:

Conceptualization: JCC

Methodology: JCC, JEP, NR, CS, AS, BAS, RHE, NRS, JSM

Investigation: JCC, JEP, NR, CS, AS, BAS

Funding acquisition: NRS, JSM

Project administration: JCC, RHE, NRS, JSM

Supervision: RHE, NRS, JSM

Writing – original draft: JCC

Writing – review & editing: JCC, JEP, NR, CS, AS, BAS, RHE, NRS, JSM

Competing interests: Authors declare that they have no competing interests

Data and materials availability: All data are available in the main text or the supplementary materials.

Supplementary Materials

Materials and Methods

Supplementary Text

Figs. S1 to S100

Tables S1 to S7

References (*45-48*)

Movies S1